2011 International Symposium on Nonlinear Theory and its Applications
NOLTA2011, Kobe, Japan, September 4-7, 2011

Multiple time-scale neurodynamics: singular perturbation, canard and chaos

Shinji Doi

Graduate School of Engineering, Kyoto University
Nishikyo-ku, Kyoto 615-8510 Japan
Email: doi@kuee.kyoto-u.ac.jp

Abstract—The classical Bonhoeffer-van der Pol (BvP) neuron model is revisited. Using rigorous asymptotic analysis, the approximate value of a bifurcation parameter in which a so-called "canard" solution appears is obtained. Interesting chaotic canard solutions generated by numerical errors and extraordinarily slow spiking are also presented. The variation of the inter-spike intervals (ISI's) and its relation to the ability of information processing in single neurons are discussed.

1. Introduction

Our brain uses spikes (action potentials) of neurons for information processing. Neuronal dynamics underlying the spike generation possess *at least* two different time scales: the fast excitatory dynamics which raise the potential quickly, and the slow recovery (refractory) dynamics [1]. Such a system with multiple time scales is a singularly perturbed system. The threshold property of neurons is produced by the multiple time scales also. So-called canard (duck) solutions play an important role in dynamical system and singular perturbation theory. In neuronal viewpoints, canard solutions are special solutions which *follow* the threshold. Therefore, canard solutions are important from the viewpoint of neuroscience.

Using the classical Bonhoeffer-van der Pol (BvP) equations of a neuron model, we explore the neuronal dynamics. We show that rigorous asymptotic analysis provide us the approximate value of a bifurcation parameter in which the canard solution appears. Interesting chaotic canard solutions of *two-dimensional* BvP model generated by computational errors are also presented. Then, extending the BvP model to three-dimensional one, we show that completely different spiking appears [2]. Finally, we investigate the variation of the inter-spike intervals (ISI's) of the model in the presence of noise and discuss its relation to single-neuronal information processing ability.

2. Simple equations for neuronal excitation (spiking)

The famous Hodgkin-Huxley (HH) equations [4] describe neuronal excitation or spike generation. The following Bonhoeffer-van der Pol (BvP) equations (or FitzHugh-Nagumo (FHN) equations) [3] are the simplified neuronal model of the HH equations:

$$\dot{x} = x - x^3/3 - y + I_{\rm ext} \quad (1a)$$

$$\dot{y} = \varepsilon(x - a) \quad (1b)$$

where $\dot{x}$ means dx/dt. The variable x denotes the membrane potential of a neuron, y is a "recovery" variable which corresponds to the combination of Na^+ inactivation and K^+ activation of the HH model, and $I_{\rm ext}$ the current stimulus applied externally.

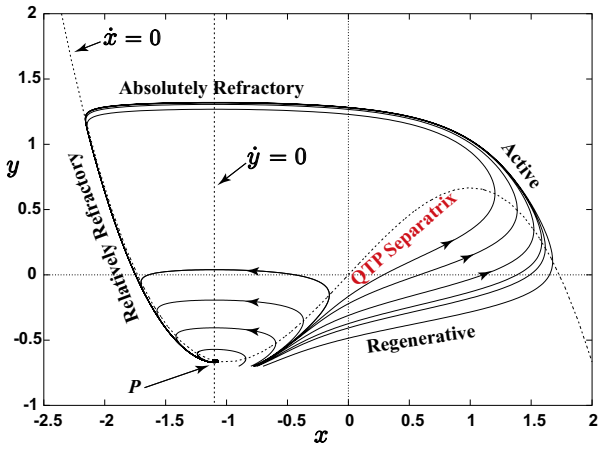

Figure 1: Phase plane of the BvP equations (1) with various orbits ($I_{\rm ext}=0, a=-1.1, \varepsilon=0.1$).

The BvP equations are a very important model which tracts the essential feature of neuronal spiking. Although the BvP model is very simple and classic, it is still interesting, particularly in the "singularly perturbed" case: $\varepsilon \ll 1$. In the following, we set as $I_{\rm ext}=0$ and change the parameter a only, since the change of $I_{\rm ext}$ has the same effect as that of a mathematically.

Let us explain the "neuronal" features of the BvP model (1). Figure 1 shows the x-y phase plane of eq. (1). The broken cubic curve is the *x-nullcline* on which $\dot{x}=0$ and the vertical broken line is the *y-nullcline* ($\dot{y}=0$). Thus, the intersection point P of the two nullclines is an equilibrium point of eq. (1) which corresponds to the resting state or the quiescent state of a neuron. Typical orbits $(x(t), y(t))$ with different initial values of eq. (1) are also drawn (corresponding waveforms of $x(t)$ are shown in Fig.2). If the neuron is in its resting state and a pulse-like current is injected, the neuron responds and settles down back to the

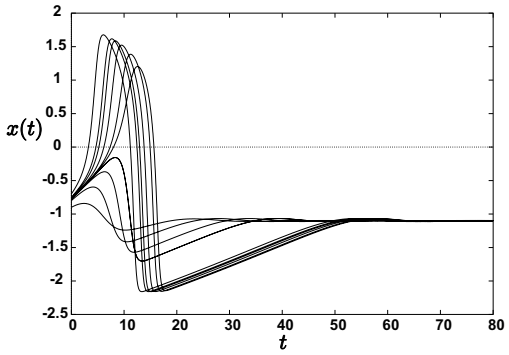

Figure 2: $x(t)$ waveforms of orbits shown in Fig.1.

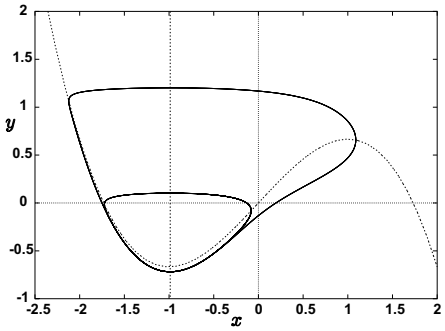

Figure 3: Large ($a = -0.98630\,13748\,30635$) and small ($a = -0.98634\,72106\,93359$) canard solutions of the BvP equations (1) ($I_{\rm ext} = 0, \varepsilon = 0.1$).

resting state after time elapse. For example, suppose that an orbit starts at the equilibrium or the resting point P. A large single-pulse perturbation in the positive (depolarizing) direction of the x-axis displaces it rightwards, it goes through both the regenerative and active regions, and finally comes back to P. If the perturbation is small, the orbit does not enter the active region, i.e. the BvP neuron model generates no spike. Note that, in Fig.1, the parameters are set as $I_{\rm ext} = 0, a = -1.1, \varepsilon = 0.1$ in which case the equilibrium point P is *stable*.

There is a curve or thin region (not shown) labeled "QTP Separatrix" near the middle branch of the cubic x-nullcline. The QTP (quasi-type) separatrix separates the "small orbit" without spike from the "large orbit" with spike in the phase plane. The word QTP denotes the fact that the separatrix does not separate the orbits in a strict sense, since the orbit continuously (but *abruptly*) changes its shape from small to large: there are intermediate orbits with medium size. The separability becomes stronger if ε is decreased. The QTP separatrix corresponds to the *quasi*-threshold of a neuron. The QTP separatrix is important not only in the viewpoint of a neuron model but also in the viewpoint of nonlinear dynamical system theory.

3. Canard solutions of the BvP equations

3.1. Asymptotic analysis of canards

If the value of a is increased from the previous value (-1.1), the y-nullcline moves rightwards and intersects with the x-nullcline in its middle branch. In this case, the equilibrium point becomes unstable, and then the BvP equations possess a stable periodic orbit (*limit cycle*).

Figure 3 shows the examples of two limit cycles for different parameter values of a. These limit cycles (in particular, the large one) are strange in a sense that it moves along the middle branch (QTP separatrix) of the x-nullcline, because the middle branch is "unstable" branch where orbits have a tendency to move away. We also note that the difference of the corresponding a values between the two limit cycles are small: a very small change of the parameter value induces a drastic change of limit cycle size. These special limit cycles are called *canards* (a French word for a duck) since their shapes remind us of a duck.

The precise value of the parameter a where the BvP equations possess a canard solution, can be obtained by using the "asymptotic analysis method" shown in [7, 8] as follows:

$$\begin{aligned} a &= a_0 + a_1\varepsilon + a_2\varepsilon^2 + a_3\varepsilon^3 + \cdots \\ & a_0 = -1,\ a_1 = \frac{1}{8},\ a_2 = \frac{3}{32},\ a_3 = \frac{173}{1024}, \\ & a_4 = \frac{7593}{16384}, \quad \cdots \end{aligned}$$

The first and second values of a shown in Fig.3 correspond to the first 5 terms and 21 terms of this asymptotic expansion, respectively.

3.2. Computer-generated chaotic canards

So far, the value of the parameter ε was 0.1. If ε is further decreased to 0.01, completely different behavior will appear. Figure 4 shows an example of the solution of eq. (1) when $\varepsilon = 0.01$. The value of a has been calculated using the first ten terms of the asymptotic expansion (Note that ten terms are enough many for numerical computation of double precision when $\varepsilon = 0.01$). The solution shows a mixed oscillation of small and large amplitudes. However, such solution is impossible in two-dimensional dynamics, since in two-dimensional phase plane, it necessarily induces intersections of the solution curve, which violate the uniqueness of solutions. The solution shown in Fig.4 is apparently chaotic one, which is also impossible in two-dimensional dynamics. Therefore, we conclude that this solution is generated by numerical errors.

As shown in Fig.1, near the middle branch of the cubic x-nullcline, there is a quasi-separatrix which separates leftward and rightward orbits in the phase plane. Canards are the special solutions which follow the "unstable" separatrix. As ε decreases, the *width* of the separatrix *exponentially* decreases. Thus, when $\varepsilon = 0.01$, the width becomes too narrow for canard solutions to follow the separatrix by

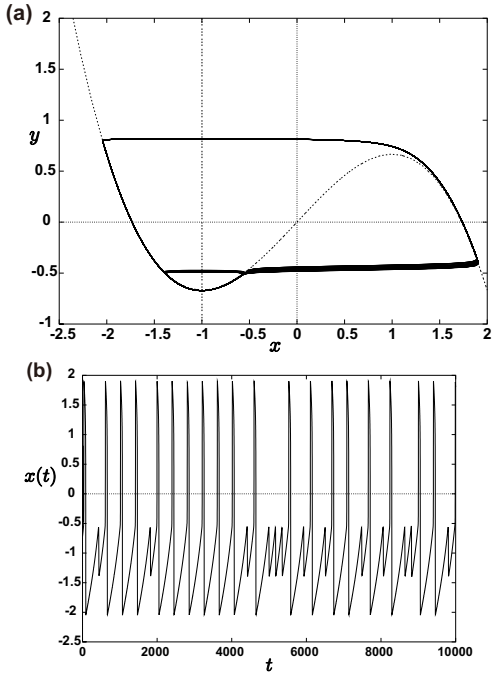

Figure 4: Chaotic canard solution generated by numerical errors. $a = -0.998704512\,45955$, $\epsilon = 0.01$, $I_{\rm ext} = 0$. **(a)** x-y phase plane. **(b)** $x(t)$ waveform.

numerical errors; numerical errors force the solution leftwards or rightwards randomly. This phenomenon shows that our asymptotic computation was very successful in obtaining such a precise value of a.

4. Extended BvP equations

In this section, we extend the BvP model (1) to three-dimensional equations [2, 5]:

$$\dot{x} = x - x^3/3 - y - z + I_{\rm ext} \quad (2a)$$
$$\dot{y} = \eta(x - ay) \quad (2b)$$
$$\dot{z} = \varepsilon(x - bz) \quad (2c)$$

Note that newly introduced equation (2c) is a simple linear equation and the variable z plays a role as an inhibitory variable since the sign of z in eq. (2a) is negative. Also note that the only nonlinear term in the equations is the cubic term in eq. (2a).

4.1. Abnormally slow spiking

Figure 5 shows the examples of *very slow* spiking in the extended BvP equations (2). The waveform of the membrane potential $x(t)$ is shown. Note that the scale of abscissa of Fig.5 is much greater than that of Fig.2: The spiking in Fig.5 is extraordinarily slow.

Between the two panels (a) and (b) of Fig.5, the behavior of spiking is much different, although both spikings are slow. In panel (a), the variable x stays in the

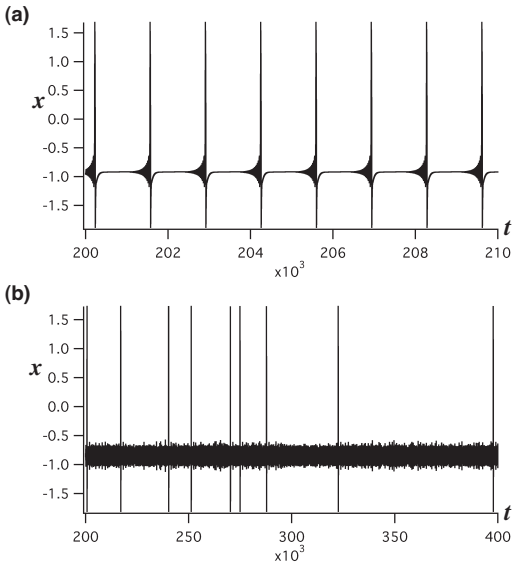

Figure 5: Examples of very slow spiking. **(a)** $a = 1.5$, $b = 1.0, \eta = 0.1, \epsilon = 0.01, I_{\rm ext} = -0.874$. **(b)** $a = 3.0$, $b = 1.0, \eta = 0.13, \epsilon = 0.01, I_{\rm ext} = -0.477175$.

neighborhood of an unstable equilibrium point without apparent oscillation and after long time elapse, it begins to make sub-threshold oscillation to make a spike finally. In panel (b), the membrane potential $x(t)$ keeps on a (chaotic) sub-threshold oscillation for a long time, and make spikes with chaotic inter-spike intervals.

4.2. Noise-Induced spiking variability

In the following, we consider the effect of noise on the BvP equations (2) and examine the inter-spike intervals (ISI's). We add a noise term $\sigma\xi(t)$ to the righthand side of (2a), where $\xi(t)$ is the Gaussian white noise (mathematically, a formal derivative of the standard Wiener process) and σ denotes the noise intensity (the standard deviation of noise).

To examine the ISI's, we consider the coefficient of variation (CV) of ISI's which is often used as a measure of spike train irregularity. The CV of a random variable T is defined using the expectation (mean) and the variance of T as ${\rm CV} \equiv \sqrt{{\rm Var}[T]}/{\rm E}[T]$.

Figure 6 shows the effect of noise on the slow spiking of the BvP equations (2). In panel (a), the mean (left axis, circle mark) and the coefficient of variation (CV, right axis, plus mark) of ISI's are plotted as a function of the noise intensity σ. Other panels show the examples of spiking (waveform of $x(t)$). The red circle and plus marks on the left axis of (a) correspond to the noiseless case ($\sigma = 0$). In this case, the neuron model shows a periodic spiking with period 1341 (dimensionless) shown in panel (b). Firstly, we note that this spiking itself is remarkable in that the spiking is extraordinarily slow as compared with the original BvP neuron model (1): the three-dimensional dynamics of the extended BvP equations is essential. Secondly, very small

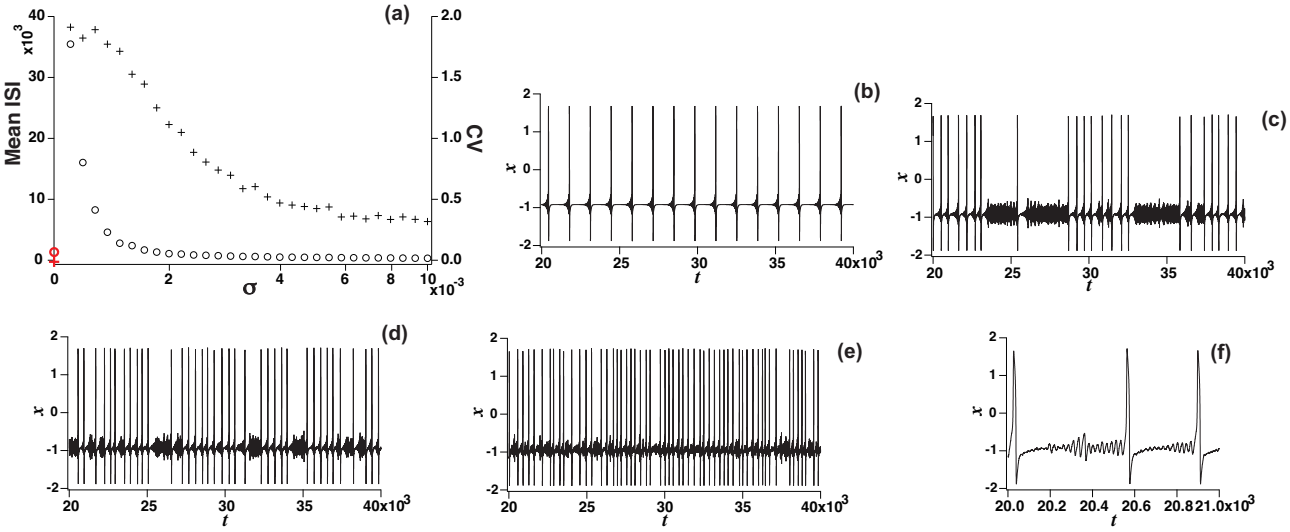

Figure 6: (a) Mean ISI (○) and CV (+) vs. noise intensity. Examples of spiking: (b) $\sigma = 0$, (c) $\sigma = 0.002$, (d) $\sigma = 0.004$, (e) $\sigma = 0.01$, (f) Magnification of (e). (a = 1.5, b = 1.0, $\eta = 0.1$, $\epsilon = 0.01$, $I_{\rm ext} = -0.874$)

noise increases the mean ISI drastically (almost forty thousands!: *noise-induced deceleration*) and the ISI variability (CV) is also high.

As the noise intensity *slightly* increases, the mean ISI changes in a wide range with the high ISI variability (high CV) remained. Recently, high ISI variability of cortical neurons attracts much attention from information encoding (see the references cited in [6]). Further increase of noise eventually induces spiking with short ISI (*noise-induced acceleration*) and moderate CV. We note that the noise intensity in Fig.6 is not so strong (see the magnification of x waveform shown in panel (f)); all phenomena are the distinct result of the interplay of noise and nonlinear dynamics of the neuron.

5. Conclusion

Using the simple BvP equations which include one nonlinear term only, we have shown several interesting nonlinear phenomena: canards, computer-generated chaos, slow oscillations near the Hopf bifurcation, noise-induced acceleration and deceleration.

From the viewpoint of neuroscience, we note that the oscillation (repetitive spiking) of BvP model is generated by the Hopf bifurcation which means that the BvP model is the class-II neuron. Regardless of this classification as the class-II neuron, the BvP neuron possess a high ability of wide-range frequency (ISI) modulation. Since ISI's are the main information carrier in our brain, the diversity of neuronal spiking presented in this paper would be important for elucidation of neuronal computation mechanism.

Acknowledgments

This work was partially supported by the Kayamori Foundation of Informational Science Advancement, the Japan Society for the Promotion of Science, and the Aihara Project, the FIRST program from JSPS, initiated by CSTP.

References

[1] S. Doi, J. Inoue, Z. Pan, K. Tsumoto, "*Computational Electrophysiology — Dynamical Systems and Bifurcations*," Springer, 2010.

[2] S. Doi, S. Kumagai, "Generation of very slow neuronal rhythms and chaos near the Hopf bifurcation in single neuron models," *J. Comput. Neurosci.* **19**, 325–356, 2005.

[3] R. FitzHugh, "Impulses and physiological states in theoretical models of nerve membrane," *Biophy. J.* **1**, 445–466, 1961.

[4] A. L. Hodgkin, A. F. Huxley, "A quantitative description of membrane current and its application to conduction and excitation in nerve," *J. Physiol.* **117**, 500–544, 1952.

[5] J. Honerkamp, G. Mutschler, R. Seitz, "Coupling of a slow and a fast oscillator can generate bursting," *Bull. Math. Biol.* **47**, 1–21, 1985.

[6] J. Inoue, S. Doi, "Sensitive dependence of the coefficient of variation of interspike intervals on the lower boundary of membrane potential for the leaky integrate-and-fire neuron model," *Biosys.* **87**, 49–57, 2007.

[7] J. Moehlis, "Canards in a surface oxidation reaction," *J. Nonl. Sci.* **12**, 319–345, 2002.

[8] J. Moehlis, "Canards for a reduction of the Hodgkin-Huxley equations," *J. Math. Biol.* **52**, 141–153, 2006.